

# Smooth Alien Species Invasion Model with Random and Time-Varying Effects

Martina Boschi

*Università della Svizzera italiana, Lugano, Switzerland.*

E-mail: [martina.boschi@usi.ch](mailto:martina.boschi@usi.ch)

Rūta Juozaitienė

*Vytautas Magnus University, Kaunas, Lithuania.*

Ernst-Jan Camiel Wit

*Università della Svizzera italiana, Lugano, Switzerland.*

**Abstract.** A species that, coming from a source population, appears in a new environment where it was not present before is named alien. Due to the harm it poses to biodiversity and the expenses associated with its control, the phenomenon of alien species invasions is currently under careful examination. Although the presence of a considerable literature on the subject, the formulation of a dedicated statistical model has been deemed essential. The objective is to overcome current computational constraints while also correctly accounting for the dynamics behind the spread of alien species.

A first record can be seen as a relational event, where the species (the sender) reaches a region (the receiver) for the first time in a certain year. As a result, whenever an alien species is introduced, the relational event graph adds a time-stamped edge. Besides potentially time-varying exogenous and endogenous covariates, our smooth relational event model (REM) also incorporates time-varying and random effects to explain the invasion rate. Particularly, we aim to track temporal variations in impacts' direction and magnitude of the ecological, socioeconomic, historical, and cultural forces at work. Network structures of particular interest (such as species' co-invasion affinity) are inspected as well.

Our inference procedure relies on case-control sampling, yielding the same likelihood as that of a logistic regression. Due to the smooth nature of the incorporated effects, we may fit a generalised additive model where random effects are also estimated as 0-dimensional splines. The consequent computational advantage makes it possible to simultaneously examine many taxonomies. We explore how vascular plants and insects behave together. The goodness of fit of the smooth REM may be evaluated by means of test statistics computed as region-specific sums of martingale-residuals.

Implementation is performed through the R package `mgcv`.

*Keywords:* relational event models, time-varying effects, random effects, generalised additive models, alien species invasions

## 1. Introduction

Each year alien species spread from a source population to a new area where they are not native, possibly employing a vector. Even though not all alien species will become invasive, this

phenomenon is now widely acknowledged as being threatening and widespread, due to the environmental change and self-perpetuating cost entailed. Its consequences on biodiversity loss, ecosystem services and human health are what make it such detrimental (McNeely, 2001).

A species is said to be introduced when it has gone beyond a great geographical barrier to reach the new location; it may then have also been established there, after overcoming challenges to survive and reproduce. Once the species has spread and proliferated, it may become invasive; in this instance, its presence is considered harmful or may cause unfavourable effects (McNeely, 2001; Pyšek and Richardson, 2010).

Comprehending the mechanisms driving the dispersal of alien species and evaluating the impact of various factors on their rate of spread are among the strategies that might assist to address this issue. Whereas some invasions are due to unaided diffusive processes, many introductions are deliberately mediated by humans for commercial and artistic purposes (Pyšek et al., 2020). Ecological, socioeconomic, historical, and cultural processes in addition to physical characteristics are some of the simultaneous forces at work. Furthermore, including and combining information on species invasiveness and region invasibility, as well as taking into consideration native and alien species already inhabiting these countries may contribute towards a more comprehensive explanation of the spread of alien species (Pyšek and Richardson, 2010).

The aforementioned drivers are intrinsically dynamic: not only do they change over time, but their influence has also been found to significantly fluctuate through time. For instance, one of the main movers of biological invasions is widely acknowledged to be international trade. A variety of goods and services, able to enhance people's lives, indeed rely on species that are native to far-off regions of the planet. The fact that temporal patterns in trade flows can be identified outlines the time-varying nature of this driver; yet, various international initiatives based on agreements and regularised border surveillance have attempted to mitigate its impact. Even if not always entirely effective, these efforts serve to clarify why trade's influence may vary over time (Hulme, 2021).

Several existing approaches attempt to describe these mechanisms. For instance, species distribution models (SDMs), a broad family of models widely used in ecology, seek to explain the presence and the abundance of a species as a response to environmental changes and to pinpoint regions that are at risk of invasion (Bellard et al., 2016). By taking into account many species at once, they have also been expanded to the community level. Despite the presence of consistent literature, the evaluation of the proper adequacy of SDMs is central. Particularly, if there is a mismatch between the geographical and temporal nature of the variables and that of the response, their ability to forecast may be deemed poor. (Araújo et al., 2019; A. Lee-Yaw et al., 2022). Given the complexity of the process and its large temporal and global scale, realistic modelling is often contentious and requires a framework that can incorporate novel components that transparently frame scientific hypotheses. In the context of social network analysis, Butts (2008) and Perry and Wolfe (2013) are responsible for developing the first formulations of relational event models (REMs), where relational events are intended as behavioural actions in which a sender and a receiver interact at a specific moment. Classical REMs rely on a considerable computational effort in the estimation procedure that, for each element of the event sequence, entails computing the sum of rates for all the couples of actors at risk of interacting at that time. This is a quantity that, in general, scales with the square of the number of individuals involved. Juozaitienė et al. (2023) interpret the time-stamped introduction of alien species as a particular relational event in which a species reaches a region in which it is not native. They

thus study their patterns by fitting taxonomic-specific REMs including random effects and able to examine the timing of invasions as well as the time-varying nature of the drivers and their impacts. On the other hand, because of how computationally costly their statistical technique is, they had to keep reducing the complexity in order to estimate the models.

In actuality, our proposal in order to understand the dynamics focuses on modelling the rate of first records, where a first record (FR) is the year in which a species is detected as alien in a region. Although the knowledge about the route and means undertaken by the species and the frequency of entrance in a nation (even if no longer with the status as alien) might be undoubtedly valuable, these pieces of information are extremely difficult to deduce or are not available. We thus refer to a global database, namely the Alien Species First Record Database, collecting information on more than 47 thousand FRs of established alien species (Seebens et al., 2018). Each record reports the year of the corresponding FR as well as the species and the region involved. We propose fitting a REM that incorporates time-varying effects and random effects in terms of smooth functions, by offering a computational edge over the models in the literature. While using our technique, we just take into account the pair species-country that invades a nation and one sampled from those who may have but did not. This computational advantage allows the inspecting of different taxonomies simultaneously. We are particularly interested in vascular plants and insects, which have been recognised as an ecologically distinct groups in terms of habitat preferences (Pyšek et al., 2010).

First, the ASFR Database's characteristics, the relatively considered subset, and the extra sources that contributed to the covariate calculation are described in Section 2. We thereafter present our model formulation involving time-varying covariates, time-varying effects and random effects in Section 3. Section 4 reports the inference technique for the estimation of these effects. Then, in Section 5, we offer a small simulation study meant to verify our statistical methodology before using it to analyse the worldwide FRs (Section 6). We conclude with a brief discussion of our work's accomplishments, as well as some of its limits and potential future paths.

Boschi et al. (2022) have previously published some of the preliminary findings of this work.

## **2. Materials**

### *2.1. Alien Species First Record Database*

The version of Alien Species First Record (ASFR) Database (Seebens et al., 2017, 2018) we are referring to in this analysis includes 47542 invasion occurrences carried out by 16922 species over 275 areas. Each row informs about a particular FR, providing the year that a species (afterwards become established) was first introduced in a certain area. Named areas are mainland countries or islands that are either frequently involved in FRs or geographically remote from the nation they are a part of politically.

Even if the time window explored by the ASFR Database is definitely larger, our analysis focuses on the period of time between 1880 and 2005. The lower limit is due to the availability of driver-related information. Nevertheless, we outline that invasion curves were almost flat before 1800: the relevance of this phenomenon has certainly risen with the onset of globalisation (Seebens et al., 2021). The upper limit is instead finalized to account for potential delays in the recording.

Our analysis focuses on two of the four most frequently cited land-based taxa, namely in-

**Table 1.** Potential drivers of Alien Species Invasions. This Table is our adaptation of the Table 1 and 2 in Juozaitienė et al. (2023) and is reporting, for each driver, the notation, the definition, the nature of the effect and the data source. Additional information may be included.

Covariate Name	Symbol	Definition	Information	Type	Data Source
<i>Distance</i>	$d_{sr}(t)$	Logarithm of the distance from the region $r$ and the nearest region invaded by species $s$ by time $t$ .	Distance between two countries is defined as the distance between their closest borders.	Time-varying covariate with time-varying effect	(Hijmans et al., 2017)
<i>Trade</i>	$tr_{sr}(t)$	Logarithm of the sum of annual trade flows (\$) between region $r$ and other countries that have been invaded by species $s$ before time $t$ .	This variable shows several missings : our imputation method is described in Section 2.2.	Time-varying covariate with time-varying effect	(Barbieri et al., 2009)
<i>Climatic Dissimilarity</i>	$dt_{sr}(t)$	Minimum difference in near-surface air temperature (in absolute value) between region $r$ and other countries that have been invaded by species $s$ before time $t$ .	—	Time-varying covariate with fixed effect	(Watanabe et al., 2011)
<i>Agricultural land-coverage</i>	$l_r(t)$	Sum of cropland and pasture proportions in the country $r$ at time $t$ .	—	Time-varying covariate with time-varying effect	(Hurt et al., 2011)
<i>Urban land-coverage</i>	$u_r(t)$	Urban area proportion in the country $r$ at time $t$ .	—	Time-varying covariate with fixed effect	(Hurt et al., 2011)
<i>Colonial ties</i>	$k_{sr}(t)$	Presence of the species $s$ at time $t$ within the colonial power to which region $r$ has belonged.	Each country is characterized either as independent or by a colonial empire it belonged to.	Time-varying covariate with fixed effect	(Becker, 2019)

sects (19 %) and vascular plants (52 %), despite the ASFR Database listing invasions involving species from 17 major taxonomic groups. Our method's computational advantage allows us to investigate the spread rate of these two taxa, simultaneously. This fact is of great interest due to the number of phenomena that involve plants and insects together, including some forms of mutualism. Mutualism can be thought as a form of cooperation between species and is recognised to have a role in facilitating the plants' introductions (Richardson et al., 2000).

## 2.2. Data on Potential Drivers of First-Record Rate

As previously indicated, the forces at work when explaining the spreading behaviour of alien species are several: the set of drivers that are taken into account in our work, their possible temporal variability, and related notation and sources are synthesized and reported in Table 1.

In practice, natural invasion episodes on the long distance seem to be relatively uncommon. In order to evaluate the role of the distance as a driver, we may take into account the shortest distance among the regions in which the species is already present at that time. *Distance* is

computed referring to the closest borders and consequently is equal to zero for neighbours. Source data for this driver consists of the R package *geosphere* (Hijmans et al., 2017). Because these data have been linked to problems with outliers in some previous analyses, we take the log-transformation into consideration.

In the existing literature, international trade has been acknowledged as a key factor for explaining the spread of alien species; furthermore, the value of import commodities is also referred to as a common proxy for the rate of alien species introductions (Seebens et al., 2018). Sometimes, the two terms are even used interchangeably (Hulme, 2021). Source information comes from Barbieri et al. (2009) and informs about the trade flow among couples of countries. The missing-value imputation procedure is worthy of attention. Juozaitienė et al. (2023) proposed an imputation method for the source data: when gaps emerge at the beginning of the observation period, they are replaced with a 0, while when the first recorded transfer between countries differs from 0, then they are imputed according to a log-linear model. The total quantity of yearly commerce between already-invaded territories and the involved region is taken into account as a covariate (*Trade*); however, occasionally, none of the countries' interested couples is mentioned for a given year. We thus decided to consider, for each couple, the trade flow at the latest year not greater than the year of interest (if the value at that time is not missing, this is the selected one). We actually outline that for several couples of regions we lack information during the years of the two World Wars. The trade volume is presumed to be equal to 0 when pair of nations is never mentioned in the data, justified by the idea that if a value is never recorded, it should be negligible. The logarithm-transformation is employed in order to account for saturation.

Bellard et al. (2016) report the climate as a relevant driver for invasions. We refer to the simulated yearly values of near-surface air temperature from Watanabe et al. (2011). We name *Climatic Dissimilarity* the minimal temperature difference between the territories in which the species was already present before the year of interest and the country to be entered in that particular year.

The proportion of cropland, pasture and urban in the land coverage (Hurt et al., 2011) are employed to assess the region's features encouraging introductions and establishment of alien species. Seebens et al. (2018) have already outlined their role in predicting the variation in first records for many taxonomic groups. We distinct *Agricultural land-coverage* and *Urban land-coverage*.

Colonial expansion, and particularly European (mainly British, but also Spanish, Portuguese and Dutch) colonialism, has been recognized to have an important role in determining the distribution of alien species (Dyer et al., 2017; Lenzner et al., 2022). Data we use come from the COLDAT structure (Becker, 2019), which informs about the presence (and the corresponding starting and ending date) of colonial powers<sup>†</sup> in the regions mentioned in Barbieri et al. (2009). In our work, each region either refers to the colonial power it belonged to or is classified as independent. Given a triplet species-region-year, the covariate *Colonial ties* assumes value 1 if the species is already present in the area of the colonial power that the invaded region belonged to and 0 otherwise.

<sup>†</sup>Belgium, Britain, France, Italy, Germany, Netherlands, Portugal, and Spain are the examined colonial powers

**Table 2.** . Main features of the final data. We report the number of the selected events from the ASFR Database between 1880 and 2005 together with the number of species and regions involved. The number of valid dyads species-region mentioned in the NR is also reported.

Taxonomic Group	N. of FR before 1880	N. of FR 1880-2005	N. of Species	N. of Countries
Insects	1098	586	114	159
Vascular plants	60448	12508	3921	120
Insects and Plants	61546	13094	4035	188

### 2.3. Native Range

A species' native range (NR) is the collection of areas where it is indigenous. In a slightly different way, we refer to NR as the set of sites where a species was already present before to the start of the observation period (in this context 1880). This notion has a central role both in ecological terms and statistical terms.

On the one hand, by reading each entry of the ASFR Database we do not learn the origin of the species; we only discover which area this species is invading. The knowledge of its NR allow us identifying which part of the world this species hails from. Additionally, fascinating relationships between the native and the invaded environments may be examined (Hejda et al., 2015).

On the other hand, in addition to being time-varying, several of the factors mentioned in Section 2.2 are also endogenous meaning that they arise from the sequence of previously occurred invasions. For each triplet species-region-year, we need understanding where the species was already present, either as alien or as native, before that time. In this sense, the notion of NR become necessary from a statistical perspective in order to compute the covariate values.

van Kleunen et al. (2019) and CABI Invasive Species Compendium (<https://www.cabi.org> accessed 15.07.2016) are some of the sources that inform on species' NRs of vascular plants and insects. In addition, the ASFR Database's invasions before 1880 were used to integrate the NRs.

Table 2 reports the structure of our final data, including the selected 13094 events between 1880 and 2005 reported in the ASFR database together with the species and the regions involved. The number of the valid dyads species-regions mentioned in the NR is also reported in Table 2.

## 3. Generative Species Invasion Model

### 3.1. Counting Process Model for Relational Events

A relational event, where a sender  $s$  interacts with a receiver  $r$  at time  $t$ , can be expressed as a triplet  $e = (s, r, t)$ . We can view this system as a network where senders and receivers are acting. The mathematical tool that we utilize to represent this system is the relational event graph  $\mathcal{G} = (\mathcal{V}, \mathcal{E})$ , where the set of nodes  $\mathcal{V}$  is composed by the set of actors and be potentially distinguished into the set of senders  $\mathcal{S}$  and the set of receivers  $\mathcal{C}$ . The time-stamped edges of this graph are the relational events themselves:

$$\mathcal{E} = \{e_k | e_k = (s_k, r_k, t_k) \subseteq \mathcal{S} \times \mathcal{C} \times T, k = 1, \dots, n_{\mathcal{E}}\}$$

Relational events can also be thought as realizations of a marked point process (MPP)  $\{[t_k, (s_k, r_k)]; k \geq 1\}$  where  $s_k \in \mathcal{S}$ ,  $r_k \in \mathcal{C}$  and  $t \in T$ , informing on the time  $t_k$  when  $(s_k \rightarrow r_k)$ .

Butts (2008) assumes that interactions, conditionally on the past, arise independently. In probability terms, the history up to an instant right before  $t$  can be thought as a filtration denoted

by  $\mathcal{F}_{t^-}$  that is function of the events that took place before time  $t$  (Perry and Wolfe, 2013; Vu et al., 2017).

We may relate a counting process (CP)  $N_{(s,r)}(t)$  to the MPP; it is counting the number of interactions  $s \rightarrow r$  in  $[0, t]$ :

$$N_{(s,r)}(t) = \{\text{n}^\circ \text{ of directed interactions } s \rightarrow r \text{ in } [0, t]\} \quad (1)$$

The following properties are assumed to hold:

- $N_{(s,r)}(0) = 0 \forall s \in \mathcal{S}, r \in \mathcal{C}$ , meaning that no event is assumed to have occurred at time 0;
- The CP  $N_{(s,r)}$  is adapted w.r.t to the increasing filtration  $\mathbb{F} = \{\mathcal{F}_t\}_{t \geq 0}$ ;
- No simultaneous events occur;

Under the above-mentioned properties, due to the non-decreasing nature of the CP, it may be declared to be a continuous submartingale and, as such, it can be decomposed in accordance to the Doob-Meyer theorem.

$$N_{(s,r)}(t) = \Lambda_{(s,r)}(t) + M_{(s,r)}(t)$$

where  $M_{(s,r)}(t)$  is a continuous martingale, and  $\Lambda_{(s,r)}(t) = \int_0^t \lambda_{(s,r)}(u) du$  is a predictable increasing process.  $\lambda_{(i,j)}(t)$  is then measurable with respect to  $\mathcal{F}_{t^-} \forall t \geq 0$ .

$$\lambda_{(s,r)}(t) dt = \mathbb{P}\{\text{interaction } s \rightarrow r \text{ occurs in } [t, t + dt)\} \quad (2)$$

We will model the intensity function  $\lambda_{(s,r)}(t)$  as a response of possibly time-varying covariates and we aim to understand the significance, the direction, and the quantification of their effects.

### 3.2. Counting Process Model for First Records

Each entry of the ASFR Database provides the essential information to interpret the alien species invasion in terms of relational event: the FR stands for the year (time) when the species (sender) first enters the new region (the receiver). As a result, each FR may be expressed as a triplet  $(s, r, t)$  and each of them consists of an observation from the MPP introduced in Section 3.1, that in this context we name invasion process (IP). The relational event graph of interest  $\mathcal{G}$  includes two kinds of nodes:  $\mathcal{S}$ , the set of species, and  $\mathcal{C}$ , the set of regions invaded, at least once, by one of the above-mentioned species between 1880 and 2005. Thus, the time-stamped edges of this relational event graph can be read as the invasion events between 1880 and 2005.

$$\mathcal{E} = \{e_k | e_k = (s_k, r_k, t_k) \subseteq \mathcal{S} \times \mathcal{C} \times T, \quad T = [1880, 2005], \quad k = 1, \dots, n_{\mathcal{E}}\}$$

Alien species invasions are non-recurrent events, namely if an introduction ( $s \rightarrow r$ ) is observed at time  $t$ , the corresponding dyad is not at risk to occur anymore. In addition, whenever an event occurs it contributes to the history of events, i.e.  $(s, r, t) \in \mathcal{F}_t$ . We remark that the history of previous events enters in the rate function through the covariates that may depend on the regions already invaded by the involved species.

We aim to model the intensity function of the CP  $N_{(s,r)}(t)$  as a response of time-varying covariates with potential time-varying effects and random effects. We will refer to the following model as Smooth Relational Event Model (Smooth REM).

$$\lambda_{(s,r)}(t|\mathcal{F}_{t^-}; \boldsymbol{\beta}(t), \boldsymbol{\theta}) = \lambda_{0g}(t) \exp \left[ \boldsymbol{\beta}(t)^T \mathbf{x}_{(s,r)}(t) + \mathbf{b}^T \mathbf{z}_{(s,r)}(t) \right] \quad (3)$$

$$\mathbf{b} \sim \mathcal{N}(\mathbf{0}, \Sigma(\boldsymbol{\theta}))$$

where:

- $\lambda_{0g}(t)$  is the non-negative baseline intensity function; its objective is to capture the residual and underlying hazard that is not explained by the drivers that are included in the model formulation. It is permitted to vary in the different classes  $g$  into which the population may be divided. For instance, in our research of interest, the baseline may differ between taxonomic groups, namely vascular plants and insects.
- $\mathbf{x}_{(s,r)}$  and  $\mathbf{z}_{(s,r)}$  are left-continuous, adapted and, thus, predictable and locally bounded covariate processes.
- $\boldsymbol{\beta}(t)$  contains the fixed or the time-varying coefficient evaluated at the corresponding time;
- $\mathbf{b}$  contains the random effects coming from a Gaussian distribution;

The choice of the elements to be included in the model specification is non-trivial. We discuss our approach in Section 6.

### 3.2.1. Endogeneous Time-Varying Covariates with possibly Time-Varying Effects

The IP is constantly evolving and, as presented in Section 2.2, the covariates, due to their endogenous nature, also change depending on its evolution. As a matter of fact, this allows keeping track of the real situation. The impact of these time-varying drivers on the rate of occurrence may be assumed to be fixed or vary over time.

Assume to deal with  $p$  fixed-effect and  $r$  time-varying-effect covariates. We can define the vector of time-varying coefficients as follows:

$$\boldsymbol{\beta}(t) = \text{diag}\{\boldsymbol{\beta}\mathbf{G}(t)\}$$

where  $\boldsymbol{\beta}$  is a  $(p+r) \times (p+r)$ -dimensional block matrix with  $(p+r)$  column partitions containing on the diagonal  $\{\boldsymbol{\beta}_1, \boldsymbol{\beta}_2, \dots\}$ ;  $\mathbf{G}(t)$  is a block matrix as well of dimension  $(p+r) \times (p+r)$  and with  $(p+m)$  row partitions. The diagonal blocks correspond to  $\{\mathbf{g}_1(t), \mathbf{g}_2(t), \dots\}$ .

If  $x_h$  belongs to the former group (fixed effect covariates), then  $\beta_h$  and  $g_h(t) = 1$  are scalar and not depending on time;  $\beta_h(t) = \beta_h$  is thus a scalar as well. If  $x_s$  belongs to the former group (time-varying-effect covariates),  $\mathbf{g}_s(t)$  is a set of radial basis functions evaluated at the time-point of interest and  $\boldsymbol{\beta}_s(t)$  coincides with the evaluation of a spline at time  $t$ . Thin plate spline may be indeed represented in terms of radial functions; nevertheless, although being extremely flexible, they necessitate estimation of a sizable number of parameters. A thin plate regression spline (TPRS) is a low-rank approximation of thin plate splines that can be incorporated in a large range of models (Wood, 2003).



### 3.2.2. Random effects

One of the goal of the study is to understand if species invasiveness and region invasibility have a significant role in increasing or decreasing the rate of occurrence of the corresponding invasion. Additionally, by examining if the presence of native as well as alien organisms implies an increased or decreased rate of invasion for other ones, we entail to explore potential dependent patterns in the spreading behaviour of species.

We thus include two kinds of random effects: the monadic random intercepts referring the involved species and territory and the dyadic random intercept that takes into account the couple composed of the invading species and the most recent species to enter the area. Due to the difference in order of magnitude of the number of insects and plants, we decided to model the species invasiveness random effect with a between-strata heteroschedasticity.

## 4. Efficient Inference Method

### 4.1. Case-Control Partial Likelihood Inference using GAMs

The estimation procedure for the unknown quantities (except for the baseline hazard function  $\lambda_{0g}(t)$  that is treated as a nuisance parameter) relies on likelihood maximization. The starting point is the observed event sequence  $\mathcal{E} = \{e_k, k = 1, \dots, n_{\mathcal{E}}\}$ , including  $n_{\mathcal{E}}$  relational events. We can switch from sequence  $\{e_k\}$  to sequence  $\{[t_k, (s_k, r_k)]\}$ , interpreted as the realizations of the MPP. By assuming the conditional independence w.r.t. to the past history, expressed as  $\mathcal{F}_{t_k^-}$ , the full likelihood can be stated as the following double product:

$$\mathcal{L}(\boldsymbol{\beta}, \boldsymbol{\theta} | \mathcal{E}) = \left[ \prod_{k=1}^{n_{\mathcal{E}}} f\{t_k | \mathcal{F}_{t_k^-}; \boldsymbol{\beta}(t_k), \boldsymbol{\theta}\} \right] \left[ \prod_{k=1}^{n_{\mathcal{E}}} \pi_{t_k}\{(s_k, r_k) | \mathcal{F}_{t_k^-}; \boldsymbol{\beta}(t_k), \boldsymbol{\theta}\} \right] \quad (4)$$

The second product is named partial likelihood (PL) (Cox, 1975). It is possible to demonstrate<sup>‡</sup> that, under the assumptions outlined in Section 3, the selection based on the knowledge that an event has occurred at time  $t_k$  follows a multinomial distribution, with the probability for each dyad  $(s_k, r_k)$  equal to the corresponding rate normalised over the sum of the rates referring to the dyads in the risk set  $\mathcal{R}_{t_k}$ , composed by the couples of actors on which an event could occur at that time.

$$\mathcal{P}\mathcal{L}(\boldsymbol{\beta}, \boldsymbol{\theta} | \mathcal{E}) = \prod_{k=1}^{n_{\mathcal{E}}} \pi_{t_k}\{(s_k, r_k) | \mathcal{F}_{t_k^-}; \boldsymbol{\beta}(t_k), \boldsymbol{\theta}\} = \prod_{k=1}^{n_{\mathcal{E}}} \frac{\lambda_{(s_k, r_k)}(t_k | \mathcal{F}_{t_k^-}; \boldsymbol{\beta}(t_k), \boldsymbol{\theta})}{\sum_{(s, r) \in \mathcal{R}_{t_k}} \lambda_{(s, r)}(t_k | \mathcal{F}_{t_k^-}; \boldsymbol{\beta}(t_k), \boldsymbol{\theta})} \quad (5)$$

Although the loss of information regarding  $\{t_k, k \geq 1\}$ , two elements make PL particularly advantageous: first, the baseline disappears, allowing the PL to exist independently of the nuisance parameter; second, the PL does not require precise timing information; rather, knowledge of the sequence of events is sufficient. Nonetheless, it is still computationally very expensive to determine the likelihood stated in (5). As previously said, for each element of the event sequence, it necessitates looking at all the possible interactions that might have happened but did not (non-events) at that time. The runtime complexity is unmanageable when the network is large enough since the size of the risk set  $\mathcal{R}(\cdot)$  is quadratic in the number of nodes.

<sup>‡</sup>Evidence can be found in Butts (2008) for the particular case of inhomogeneous Poisson processes, but the result can be generalized for the above-mentioned assumptions.

Nested case-control (NCC) sampling (Borgan et al., 1995; Lerner and Lomi, 2020) considers, for each event in the sequence  $\mathcal{E}$ , a reduced risk set being composed of the case  $(s, r)$  and  $m - 1$  controls, sampled according to a given probability distribution  $\pi_t(\cdot|(s, r))$ . We just consider two components of the risk set: the dyad taking part in the event and one randomly sampled among those possibly (but in actuality not) engaging at that time; for doing inference we thus consider NCC sampling with  $m = 2$ .

We may refer to a new MPP  $\{[t_k, [(s_k, r_k), SR_{t_k}]] ; k \geq 1\}$  where  $SR_{t_k}$  is the sampled risk set (SR) at time  $t_k$ , whose marked space follows:

$$E = \{[(s, r), \mathbf{sr}], s \in \mathcal{S}, r \in \mathcal{C}, \mathbf{sr} \in \mathcal{P}_{(s, r)}\}$$

If  $\mathcal{P}$  is the power set of all the possible pairs  $(s, r)$ , where  $s \in \mathcal{S}$  and  $r \in \mathcal{C}$ , we define  $\mathcal{P}_{(s, r)}$  as its subset containing  $(s, r)$ . In particular, when  $m = 2$  we focus on the subset of  $\mathcal{P}$  including  $(s, r)$  and one other dyad only.

As in the previous case, we can associate a CP  $N_{[(s, r), \mathbf{sr}]}(t)$ :

$$N_{[(s, r), \mathbf{sr}]}(t) = \sum_{k \geq 1} I\{t_k \leq t, [(s_k, r_k), SR_{t_k}] = [(s, r), \mathbf{sr}]\} \quad (6)$$

where the CP in Equation (1) can be retrieved as:

$$N_{(s, r)} = \sum_{\mathbf{sr} \in \mathcal{P}_{(s, r)}} N_{[(s, r), \mathbf{sr}]}$$

It is necessary to consider a new filtration  $\mathcal{H}_t = \mathcal{F}_t \cup \sigma\{SR_{t_k}; t_k \leq t\}$ , that consists of the the cohort history augmented with the sampling information. We work under the assumption of independent sampling, meaning that sampled controls have the same failure risk as non-selected ones. Under this assumption, the intensity process of the CP  $N_{(s, r)}$  is adapted not only to  $\mathbb{F}$  but also to  $\mathbb{H} = \{\mathcal{H}_t\}_{t \geq 0}$  (Borgan and Zhang, 2015).

We can decompose the intensity process of the CP  $N_{[(s, r), \mathbf{sr}]}(t)$  in two different ways:

$$\begin{aligned} \lambda_{[(s, r), \mathbf{sr}]}(t) &= \lambda_{(s, r)}(t) \pi_t(\mathbf{sr}|(s, r)) \\ &= \lambda_{\mathbf{sr}}(t) \pi_t((s, r)|\mathbf{sr}) \end{aligned}$$

On the one hand, in the case of NCC sampling with  $m = 2$ ,  $\pi_t(\mathbf{sr}|(s, r))$  is equal for all the couples in  $\mathbf{sr} \subset SR_t$ .

$$\pi_t(\mathbf{sr}|(s, r)) = [n(t) - 1]^{-1} \cdot I\{(s, r) \in \mathbf{sr}, \mathbf{sr} \subset \mathcal{R}_t, |\mathbf{sr}| = 2\} \quad (7)$$

where  $n(t)$  is the number of dyads at risk at  $t$ . Whenever we deal with a stratified REM, such as in Equation 3, we may refer to Borgan and Langholz (1997) and constraint the sampling of controls being part of the same stratum as the case. If we match the control with the case (matched NCC), then  $n_g(t) \leq n(t)$  represents the cardinality of the subset of the risk set containing the dyads of stratum  $g$  at risk.

On the other hand, the probability that the couple  $(s, r)$  interacts at  $t$  given  $\mathcal{H}_{t-}$  and that  $(s, r) \in \mathbf{sr}$  is equal to:

$$\pi_t((s, r)|\mathbf{sr}, \mathcal{H}_{t-}) = \frac{\lambda_{[(s, r), \mathbf{sr}]}(t|\mathcal{H}_{t-})}{\lambda_{\mathbf{sr}}(t|\mathcal{H}_{t-})} \quad (8)$$

By considering the joint product of probabilities in Equation (8), we can retrieve a new PL, named sampled PL:

$$\begin{aligned} \mathcal{P}\mathcal{L}_S(\boldsymbol{\beta}, \boldsymbol{\theta} | \mathcal{E}) &= \prod_{k=1}^{n_{\mathcal{E}}} \frac{\lambda_{(s_k, r_k)} \left[ t_k | \mathcal{H}_{t_k}^-; \boldsymbol{\beta}(t_k), \boldsymbol{\theta} \right] \pi_{t_k} \left[ SR_{t_k} | (s_k, r_k) \right]}{\sum_{(s, r) \in SR_{t_k}} \lambda_{(s, r)} \left[ t_k | \mathcal{H}_{t_k}^-; \boldsymbol{\beta}(t_k), \boldsymbol{\theta} \right] \pi_{t_k} \left[ SR_{t_k} | (s, r) \right]} \\ &= \prod_{k=1}^{n_{\mathcal{E}}} \frac{\exp \left[ \boldsymbol{\beta}^T(t_k) [\mathbf{x}_{(s_k, r_k)}(t_k) - \mathbf{x}_{(s_k^*, r_k^*)}(t_k)] + \mathbf{b}^T [\mathbf{z}_{(s_k, r_k)}(t_k) - \mathbf{z}_{(s_k^*, r_k^*)}(t_k)] \right]}{1 + \exp \left[ \boldsymbol{\beta}^T(t_k) [\mathbf{x}_{(s_k, r_k)}(t_k) - \mathbf{x}_{(s_k^*, r_k^*)}(t_k)] + \mathbf{b}^T [\mathbf{z}_{(s_k, r_k)}(t_k) - \mathbf{z}_{(s_k^*, r_k^*)}(t_k)] \right]} \end{aligned} \quad (9)$$

where  $(s_k^*, r_k^*)$  is the dyad randomly sampled from  $\mathcal{B}_{t_k}$ .

Expression (9) is not only computationally less expensive to get, but it can also be proved to correspond to the likelihood of a generalised linear mixed model (GLMM) without intercept for binary outcomes, where the observed response is equal to 1 for all the observations and the covariates are assessed as the difference between those associated with the event and those computed for the randomly sampled non-event. The probabilist component leading this GLMM is stated as follows:

$$\begin{aligned} &Y_k | \mathbf{x}_{(s_k, r_k)}(t_k), \mathbf{x}_{(s_k^*, r_k^*)}(t_k), \mathbf{z}_{(s_k, r_k)}(t_k), \mathbf{z}_{(s_k^*, r_k^*)}(t_k), \mathbf{b} \stackrel{i.i.d}{\sim} \\ &\text{Ber} \left( \pi_k = \frac{\exp \left[ \boldsymbol{\beta}(t_k)^T [\mathbf{x}_{(s_k, r_k)}(t_k) - \mathbf{x}_{(s_k^*, r_k^*)}(t_k)] + \mathbf{b}^T [\mathbf{z}_{(s_k, r_k)}(t_k) - \mathbf{z}_{(s_k^*, r_k^*)}(t_k)] \right]}{1 + \exp \left[ \boldsymbol{\beta}(t_k)^T [\mathbf{x}_{(s_k, r_k)}(t_k) - \mathbf{x}_{(s_k^*, r_k^*)}(t_k)] + \mathbf{b}^T [\mathbf{z}_{(s_k, r_k)}(t_k) - \mathbf{z}_{(s_k^*, r_k^*)}(t_k)] \right]} \right) \end{aligned} \quad (10)$$

$k = 1, \dots, n_{\mathcal{E}}$

Since Equation (9) may be expressed as the likelihood of a GLMM for binary outcomes and due to the specification we supplied in Section 3.2 for the time-varying effects, we may obtain the the estimated parameters of interest by fitting a generalised additive model (GAM), including two different types of smooth terms:

- Time-varying effects are modelled as TPRS;
- Random effects may be estimated as smooth terms of dimension 0 whose basis functions take value 1 in the presence of the appropriate level of the random factor and 0 otherwise.

We consequently need to add a penalization term to the sampled PL in Equation (9), depending on the penalty matrices related to the included splines. Particularly, random effects supposed to be *i.i.d.* normally distributed – as stated in our model formulation in Equation (3) – arise from a penalty that consists of an identity matrix of dimension equal to the number of levels of the corresponding random factor (Pedersen et al., 2019).

The previously exposed inference technique is implemented by using the R package `mgcv` (Wood, 2003; Wood et al., 2016; Wood, 2017).

We consider, for sake of simplicity, a unique vector of estimated coefficients  $\hat{\boldsymbol{\gamma}}(t) = \begin{bmatrix} \hat{\boldsymbol{\beta}}(t) & \hat{\mathbf{b}} \end{bmatrix}$  referring to the covariate process  $\mathbf{v}_{(s, r)}(t) = [\mathbf{x}_{(s, r)}(t) \quad \mathbf{z}_{(s, r)}(t)]$ . By replacing the estimates in the cumulative intensity process  $\Lambda_{(s, r)}(t)$  we are able to define the Martingale residuals:

$$\hat{M}_{(s, r)}(t) = N_{(s, r)}(t) - \hat{\Lambda}_{(s, r)}(t)$$

#### 4.2. Non-Parametric Estimation for the Baseline Hazard Function

The cumulative baseline function  $\Lambda_0(t) = \int_{t_0}^t \lambda_0(u) du$  may be estimated non-parametrically. In particular, we refer to Borgan et al. (1995) and Borgan and Langholz (1997) that propose an adaptation of the Breslow estimator for sampled cohort data.

$$\hat{\Lambda}_0(t | \mathcal{H}_{t^-}; \hat{\boldsymbol{\gamma}}(t)) = \sum_{t_k \leq t} \frac{1}{\sum_{(s,r) \in SR_{t_k}} \exp[\hat{\boldsymbol{\gamma}}(t)^T \mathbf{v}_{(s,r)}(t)] w_{(s,r)}(t_k, SR_{t_k})} \quad (11)$$

where:

$$w_{(s_k, r_k)}(t, \mathbf{s}r) = \frac{\pi_t(\mathbf{s}r | (s_k, r_k))}{n(t)^{-1} \sum_{(s,r) \in \mathbf{s}r} \pi_t(\mathbf{s}r | (s, r))}$$

Since we deal with matched NCC with  $m = 2$  and with a stratification of the population, we can define the group-specific estimator of the cumulative baseline hazard,  $\Lambda_{0g}(t)$ , as follows:

$$\hat{\Lambda}_{0g}(t | \mathcal{H}_{t^-}; \hat{\boldsymbol{\gamma}}(t)) = \sum_{t_k \leq t: (s_k, r_k) \in g} \frac{1}{\sum_{(s,r) \in SR_{t_k}} \exp[\hat{\boldsymbol{\gamma}}(t)^T \mathbf{v}_{(s,r)}(t)] \frac{n_g(t_k)}{2}} \quad (12)$$

where  $n_g(t)$  has been defined in the context of Equation (7). Equation (12) will be referred as matched estimator for the baseline hazard. Nonetheless, in some circumstances, one may opt for a pooled estimation, obtained starting from Equation (11) and assigning a probability equal to 0 to those SR made of dyads that do not belong to the same stratum as the case.

#### 4.3. Goodness of Fit Evaluation

Although the presence of a relevant literature on REMs, evaluating their fit's adequacy to the data is still a contentious subject (Brandenberger, 2019). On the one hand, conventional approaches for the Cox Proportional Hazard Model, including the evaluation of Schoenfeld, Deviance and Martingale residuals have been expanded to Cox Mixed Effect Models. On the other hand, Brandenberger (2019) has proposed an approach aimed at simulating a portion of the event sequence and comparing the simulated and really-occurred relational events. The guiding principle behind this technique is that the former should resemble the latter if the model fits the relational events well, especially if the model incorporates all the relevant network dynamics. Although, this method is computationally costly and relies on several assumptions as well.

Lin et al. (1993); Borgan and Zhang (2015) introduce, for the Cox Proportional Hazard Model, a variety of methods based on the cumulative sum of martingale residuals, that can be used in the presence of time-varying covariates as well. Due to the presence of time-varying effects in our model formulation, that lead explicitly to the violation of the proportional hazard assumption, our proposal relies on the goodness of fit tools presented in Marzec and Marzec (1997) and Marzec and Marzec (1998).

Specifically, we rely on a zero-mean Martingale-residual type process, obtained by stratifying according to the receiver involved in the relational events. We can read it as a weighted sum of martingale residuals:

$$G_{r^0}[\hat{\boldsymbol{\gamma}}(t), t] = \int_0^t \sum_{k=1}^{n_g} \left[ I[r_k = r^0] - \frac{\Phi_{r^0, \mathbf{s}r}^{(0)}[\hat{\boldsymbol{\gamma}}(u), u]}{S_{\mathbf{s}r}^{(0)}[\hat{\boldsymbol{\gamma}}(u), u]} \right] dN_{(s_k, r_k)}(u) = \int_0^t \sum_{k=1}^{n_g} I[r_k = r^0] d\hat{M}_{(s_k, r_k)}(u) \quad (13)$$

where  $r^0$  is a particular receiver in  $\mathcal{C}$ ,  $\Phi_{r^0, sr}^{(0)}[\boldsymbol{\gamma}(t), t] = \sum_{(s,r) \in sr} I[r = r^0] \cdot \exp[\boldsymbol{\gamma}(t)^T \mathbf{v}_{(s,r)}(t)] \cdot \pi_t(sr|(s,r))$  and  $S_{sr}^{(0)}[\boldsymbol{\gamma}(t), t] = \sum_{(s,r) \in sr} \exp[\boldsymbol{\gamma}(t)^T \mathbf{v}_{(s,r)}(t)] \cdot \pi_t(sr|(s,r))$ .

Specifically, as a test-statistic, we consider the standardized recipient-specific process in Equation (13) evaluated at the last time point of each event sequence  $\tau$ , that may be proved to behave as a standard normal asymptotically.

$$\frac{G_{r^0}[\hat{\boldsymbol{\gamma}}(\tau), \tau]}{\sqrt{\langle G_{r^0}[\hat{\boldsymbol{\gamma}}(\tau), \tau], G_{r^0}[\hat{\boldsymbol{\gamma}}(\tau), \tau] \rangle}} \xrightarrow{D} N(0, 1) \quad n \rightarrow \infty \quad (14)$$

where  $\langle \cdot, \cdot \rangle$  refers to the predictable covariation.

## 5. Simulation Study

We provide a brief simulation to validate our parametric methodology for quantifying the potentially time-varying effects of drivers, our non-parametric technique for evaluating the baseline hazard function and our strategy for assessing the goodness of fit. The aim of this study is to generate data that is similar to what has been observed in practise. To achieve this goal, we first fit a basic model including *Distance* and *Climate Dissimilarity* on insect invasions, obtaining estimates for the time-varying effect of the former and fixed effect of the latter. We account for these estimates as the true value for the parameters leading the intensity of the simulated IPs. Each of them creates the year in which insects invade countries for the first time.

At the beginning of the observational period, in our case the year 1880, the risk set  $\mathcal{R}_{1880} \subset \mathcal{S} \times \mathcal{C}$ , where  $\mathcal{S}$  is the set of insect-species that have been introduced as alien in at least one region between 1880 and 2005 and  $\mathcal{C}$  is set of countries invaded at least once by those species in the same period. Couples species-regions that are mentioned in the native range are not included in the risk set.

We name  $\Delta T_{(s,r)}$  the inter-arrival time until  $(s \rightarrow r)$  occurs from the last occurred event  $t^-$ . Then, for dyads in  $\mathcal{R}_t$ ,  $t^- + \Delta T_{(s,r)} \geq t$ . For simplicity, we assume that the time  $\Delta T_{(s,r)}$  behaves as an Exponential distribution with a time-varying rate  $\lambda_{(s,r)}(t|\mathcal{F}_{t^-})$ .

Specifically, the true intensity of the underlying IP is defined as follows:

$$\lambda_{(s,r)}(t|\mathcal{F}_{t^-}) = \lambda_0(t) \exp[\beta_1 \cdot dt_{sr}(t) + \beta_2(t) \cdot d_{sr}(t) + b_{ins} \cdot I(s = ins) + b_{reg} \cdot I(r = reg)]$$

where  $\beta_1(t), \beta_2(t), b_{ins}, b_{reg}$  are the estimate from the fitting of the smooth REM on the real data involving insects. The true value of  $\lambda_0(t), t \in [1880, 2005]$ , common for all the dyads under study, is assumed to be proportional to the absolute value of a spline function fitted to the following ratio:

$$\frac{\text{N}^\circ \text{ of observed events at time } t}{\text{N}^\circ \text{ of dyads at risk at time } t}$$

where  $t$  is an event time observed in the real data.

In practice, we will observe the faster interarrival-time among the possible ones; the minimum among Exponentially distributed random variables still behaves as an Exponential random variable.

$$\Delta T = \arg \min_{(s,r) \in \mathcal{R}_t} \Delta T_{(s,r)} \sim \text{Exponential} \left( \sum_{(s,r) \in \mathcal{R}_t} \lambda_{(s,r)}(t|\mathcal{F}_{t^-}) \right)$$

Nevertheless, the Exponential is a continuous distribution; on the contrary, we deal with a discrete-nature piece of time information that consists in the year of the occurred event. Additionally, due to the nature of the drivers, we are able to update the hazard rate only at discrete years. For this reason, every time we simulate a new event time  $t$ , we need evaluate if its floor (namely, the greatest integer less than or equal to  $t$ ) is larger than the last year for which the hazard has been updated. If it is the case, we proceed to update the hazard and we do not sample any event, otherwise the dyad involved in the invasion is sampled.

Conditionally to the new invasion time  $t$ , we consider a random variable  $D$  that may assume one value among the dyads in the risk set at time  $t$ , according to a multinomial distribution.

$$P[D = (s, r)|t] = \frac{\lambda_{(s,r)}(t|\mathcal{F}_{t-})}{\sum_{(s',r') \in \mathcal{R}_t} \lambda_{(s',r')}(t|\mathcal{F}_{t-})}$$

Once we deal with a new simulated FR, the triplet  $(s, r, t)$  is removed from the risk set and integrates the history of events  $\mathcal{F}_t$ . The simulation procedure continues until the year 2005.

We simulated 50 different IPs according to Algorithm 1 (reported in the Supplementary Materials) and for each of them:

- (a) We build a case-control data set, with a number of rows equal to the number of simulated events, a column composed by fixed values equal to 1 and reporting, for each event  $e_k = (s_k, r_k, t_k)$ , a dyad  $(s_k^*, r_k^*)$  randomly sampled from  $\mathcal{R}_{t_k}$ . It also reports, for each row, the difference between the values of the covariates *Distance* and *Climatic Dissimilarity* computed for the dyads  $(s_k, r_k)$  and  $(s_k^*, r_k^*)$  at time  $t_k$ . We remark that in order to fit the model in Equation (3) as a GAM, we need to structure the data adequately, as described above. This data structure is built for real data as well.
- (b) A GAM following the probabilistic component in Equation (10) can thus be fitted to each of the case-control data sets.
- (c) The fitted  $\hat{\boldsymbol{\gamma}} = \{\hat{\beta}_1, \hat{\beta}_2(t), \hat{b}_{ins}, \hat{b}_{reg}\}$  are used to estimate the baseline hazard function according to the estimator shown in Equation (11).
- (d) The behaviour of the test-statistic in Equation (14) has been studied for each simulation.

Figures 1 *Up-Right* and *Up-Left* show that our procedure achieves optimal results in terms of accuracy of the parametric estimate of covariates' effect. Instead, we can see that our model tend to slightly overestimate the standard deviations of the random effects. From Figure 2, on the other hand, one can notice that estimates for cumulative baseline hazard are less precise. Yet, the tendency of the curve is appropriately detected. Finally, estimated densities fitted on the standardised martingale residual processes computed at the end of the observational period for the involved regions behave closely to a normal distribution, as shown in Figure 3, that is the result we expect in the presence of good fitting of the model to the data.

## 6. Analysis of Alien Species First Records

One of the main goal of this paper consists in deepening which are the forces that move alien species invasions, by properly accounting for the time-dimension and the relationships between invasive and previously established species. Because of our technique's computational advantage, we inspect a relational event network including more than one taxonomy at the same time.

We particularly focus on insects and plants due to the large number of phenomena that make the relationship between these two taxa of particular interest, such as, for instance, mutualisms. Mutualisms may have several forms such as protection (in return for guard against herbivores, plants evolve particular traits features to shelter and nourish insects) and pollination (strengthen features of the plants attract the insects that successively play the role of vectors for the transport of their pollen). Mutualisms between plants and insects seem to have a role in alien species invasions and particularly to accelerate their spread (Prior et al., 2015; Simberloff and Von Holle, 1999). The term invasional meltdown has been introduced for underlying how non-indigenous species may collaborate in order to increase the probability of success of the invasive process with respect to that they may have by acting alone. For instance, non-native plants and insects may cause variations in their habitats in order to enhance other non-indigenous species to be introduced and established in these areas.

To formalise alien plant and insect invasions, we refer to a relational event graph, where the group of senders  $\mathcal{S}$  may be separated into two different types of nodes: the ensemble of insects  $\mathcal{S}_{ins}$  and the set of vascular plants  $\mathcal{S}_{plt}$ . As a species invades a country, a time-stamped directed edge arises toward one of the nodes in the collection of countries  $\mathcal{C}$ . Following Borgan and Langholz (1997), we stratify our model using the taxonomy of the species involved, namely  $g \in \{ins, plt\}$  in Equation (3). In addition to the drivers reported in Table 1, species' invasiveness and regions' popularity, we further take into account, for each recorded occurrence  $(s_k, r_k, t_k)$ , the interaction species-last species  $s_k \cdot s'_{r_k}(t_k)$  and  $s_k^* \cdot s'_{r_k^*}(t_k)$  evaluated for the event and non-event. The last species  $s'_{r_k}(t_k)$  and  $s'_{r_k^*}(t_k)$  arrived before time  $t_k$  in regions  $r_k$  and  $r_k^*$ , respectively<sup>§</sup>. We point out that species and last species, in this context, may be members of separate taxonomies, allowing us to deepen the intriguing relationships between insects and vascular plants.

Model selection has been conducted by evaluating the corrected version of AIC (Wood et al., 2016). This correction, relying on the adjustment for the degrees of freedom, allows avoiding the tendency to chiefly select the simplest or the more complex model. Figure 4 shows the values of AIC for the 63 evaluated model formulations, including different subsets of the covariates shown in Table 1. Following Juozaitienė et al. (2023), whenever included, *Distance*, *Trade* and *Agricultural Land-Coverage* have a time-varying effect, while *Climatic Dissimilarity*, *Urban Land-Coverage* and *Colonial ties* are supposed to remain constant over time. The best model according to corrected AIC includes *Distance*, *Trade*, *Colonial Ties* and *Difference in Temperature*. According to the hypothesis testing on the single drivers, all of them are revealed to have a significant effect.

Land-cover characteristics seeming to have no impact on the dynamics of invasions is the first factor we may assess. Particularly, as it is possible to observe in Figure 4, the presence of these variables implies an increase in the value of AIC.

Both the fixed coefficients, related to the climatic conditions and to the spread of the colonialism turn out to be negative. The former result is quite intuitive: if a species has already invaded nations with a comparable temperature, the pace of invasions tends to rise. The latter instead is counter-intuitive; we expected that the presence of the species in the regions of some colonial power would have increase the probability of invading a country belonging to the same

<sup>§</sup>These two entries may assume the categories *Rare interaction* and *Novelty* as well. The former is used when the species-last species interaction appears only once among those recorded for events and non-events; the latter is taken into account if no other species are detected in the related country before the considered time.

power. Nevertheless, we outline a positive correlation between *Colonial Ties* and *Trade* that may have determined this unexpected result.

Time-varying coefficients related to distance are negative, initially reducing and subsequently growing (in absolute value). This fact confirms how unusual long-distance natural invasion occurrences are. On the contrary, albeit with a fading effect over time, the significant and positive impact of trade on alien species invasions is confirmed. This tendency has already been discussed in the literature, motivated by the fact that the percentage of traded goods with an important impact on alien species invasions is decreasing (Juozaitienė et al., 2023); in this sense, the impact of trade is diminishing because its nature is evolving. Additionally, the augmented control at the borders may have led to a decrease of the effect of this driver. The time-varying of trade and distance are depicted in Figure 5 as smooth functions of time. Also included are the corresponding posterior confidence intervals.

Once the fixed and the time-varying effect of the covariates are properly accounted for, we may look to the largest estimated values of the random effects related to the insect and plant invasiveness. *Frankliniella occidentalis*, the most invasive insect found, has a long history of foreign species incursions dating back to the 1970s. It is widely known for its pest qualities and ability to cause significant plant harm (Kirk and Terry, 2003). Another largely invasive species is *Anoplolepis gracilipes*, a very small ant, which is able to negatively impact on the native ecosystems, particularly on forests. On the other hand, among the most invasive plants represented in Figure 7, we can identify *Chromolaena odorata*. While its effect in South Africa have been largely studied and need to be controlled, it also has beneficial effect in central Africa. Insect and plant invasiveness random effects are assumed to come from two independent Gaussian distributions. The retrieved standard deviations are in practice of two different order of magnitude (1.86 and 0.31, respectively). On the other side, Figure 6 aims to depict the region's invasibility in terms of random effects. The fact that the two most popular ones, namely Australia and Canada, belonged to the British power supports the literature already in existence (Juozaitienė et al., 2023). Estimated coefficients – we remark that in this context random effects are estimated as coefficients of a 0– dimensional splines – related to South Africa, United States, and New Zealand are positive as well, meaning that the probability of alien species invasion is larger in these areas.

Figure 7 illustrates the greatest co-invasion relationships between species. Particularly, we are interested in determining whether the presence of a, native or alien, species affects the likelihood of an invasion event occurring or not. It is intriguing to witness interactions between species that pertain to different taxa: for instance, we can see that a positive random effect is estimated for *Phenacoccus manihoti* (commonly known as cassava mealybug) when *Chromolaena odorata* (Siam weed) has reached the country. The reader may find of interest that the research by Calatayud et al. (1994), aimed to explore variations in the dynamics of *P. manihoti* in relation to seasonality and some relevant substances, has been conducted in Brazzaville (Congo), where *C. odorata* was the primary plant species. The opposite tendency is estimated (negative random effect) for *Frankliniella occidentalis* (western flower thrip) invading a region reached by *Achyranthes aspera* (chaff-flower). We can find in the literature two instances where the aforementioned weed seem related to viruses whose transmission *F. occidentalis* may be involved. Particularly, *A. aspera* is specifically mentioned by Kumar et al. (2008) as being a part of the *Tobacco Streak Virus*' native range. Because of the harm caused by this virus, one potential response may be the development of a resistance, which has actually been observed in



a plant that is resistant to *F. occidentalis*. Additionally, Macharia et al. (2016) analysis of the plants in the tomato production area in Kenya revealed the presence of *A. aspera*. However, it is unclear how it might act as a host for the *Tomato spotted wilt virus*, for which *F. occidentalis* is a renowned vector.

Once all the previous features have been taken into account, we may inspect the estimated cumulative baseline hazard. In Figure 8, one can find the estimates according to Equation (12). The shape of the curve for insects suggests that the rate of invasions for this taxonomy is growing in a way that the model's built-in drivers are unable to account for. Yet, for vascular plants, the existence of a linear estimated function may be interpreted as a constant underlying baseline. This result confirms the literature (Bonnamour et al., 2021). They outline the largest increase in the rate for insects comparing to plants. Particularly, they claim that different scale is due to the fact that insects took more advantage from the availability of fast transportation tools rather than plants, already able to survive for longer time across journeys. Furthermore, due to the smaller dimension of insects and to their mobility, insects may also be harder to identify (Walliser, 2013) and thus to be completely explained by a proper set of covariates.

As previously introduced, we aim to evaluate the region-specific standardized sum of Martingale residuals for each element in  $\mathcal{C}$  according to expression (14). The distribution of our test statistic under the null of adequacy of the model is known and asymptotically normal.

Since we implement a sort of multiple testing, we refer to the false discovery rate (FDR) correction of the p-values. Considering the classical p-values, the Norway-, Australia-, United Kingdom-, Canada- and Hawaiian Islands- test statistic lead to a rejection. By instead evaluating the FDR correction of the p-values, none of them is smaller than 5%.

## 7. Discussion

The smooth REM allowed us to improve the explanation of the dynamics driving alien species invasions, by incorporating time-varying and random effects in the model formulation. Dealing with drivers whose effects change over time is indeed quite typical in practice, especially if the observational time is fairly long as in this context where it covers more than one century. The inclusion of such effects allowed us to understand that the impact of one of the most relevant drivers of alien species invasions is actually decreasing. One may additionally deepen its impact, by adding to the model an interaction effect between *Trade* and *Colonial Ties*. From another perspective, random effects enable us to track the actors involved in the current and previously occurred events by incorporating network activities. The range of network dynamics that random factors might depict might be broadened. We have just included monodic and dyadic random effects in our approach. Particularly, the alien species relational event graph is bimodal, precluding the appearance of triadic network dynamics.

Our estimation method relies on the sampled PL, which considers in the risk set at each time only one event and non-event. We gain, in this way, a computational advantage. In particular, the computational effort in a Cox Proportional Hazard Model dealing with splines and relying on the partial likelihood in Equation (5) scales with  $n_{\mathcal{E}} \times n_{\mathcal{J}} \times n_{\mathcal{C}} \times d^3$ , where  $d$  is the number of predictors involved in the model formulation. Instead, case-control partial likelihood via GAMs scales with  $n_{\mathcal{E}} \times d^3$ . We remark that, due to implementation constraints, we were not able to fit a model with  $d > n_{\mathcal{E}}$ . For this reason, in our study, when considering the species co-invasion network structure, we did not include all the possible levels that this variable assume in observed

events and non-events but we codified dedicated categories. Nevertheless, as a future direction for our efficient technique, we propose sampling more than one non-event for each observed instance. This additional non-event sampling procedure does not change the formalization of the technique. Instead of only once, the observed occurrence is repeated  $m - 1$  times, each record with a different sampled non-event. Each of them is then weighted  $\frac{1}{m-1}$ . According to this expansion of the method, we are able to increase the number of listed events  $n_{\mathcal{E}}$ . At the same time, in presence of random factors with potential large number of levels, we expect to observe more of these levels (leading to an increase of  $d$ , as well). Concerning the goodness of fit, we outline that although referring to an asymptotic result, some of the countries are invaded only a small number of times. Additionally, in the Supplementary Materials, it is possible to find the evaluation of a species-specific test statistic: insects and plants empirical distribution of the statistics are evaluated separately.

We conclude by claiming that our model does not include, for the moment being, a potential relevant information, namely the sampling frequency. Particularly, due to the technical and scientific improvement of species recording, a larger range of species might have been discovered over time. Including a covariate accounting for the number of instances detected by year and by country should improve the inspection of the dynamics of interest (Bonnamour et al., 2021).

## References

- A. Lee-Yaw, J., L. McCune, J., Pironon, S. and N. Sheth, S. (2022) Species distribution models rarely predict the biology of real populations. *Ecography*, **2022**, e05877.
- Araújo, M. B., Anderson, R. P., Márcia Barbosa, A., Beale, C. M., Dormann, C. F., Early, R., Garcia, R. A., Guisan, A., Maiorano, L., Naimi, B. et al. (2019) Standards for distribution models in biodiversity assessments. *Science Advances*, **5**, eaat4858.
- Barbieri, K., Keshk, O. M. and Pollins, B. M. (2009) Trading data: Evaluating our assumptions and coding rules. *Conflict Management and Peace Science*, **26**, 471–491.
- Becker, B. (2019) Colonial Dates Dataset (COLDAT). URL: <https://doi.org/10.7910/DVN/T9SDEW>.
- Bellard, C., Leroy, B., Thuiller, W., Rysman, J.-F. and Courchamp, F. (2016) Major drivers of invasion risks throughout the world. *Ecosphere*, **7**, e01241.
- Bonnamour, A., Gippet, J. M. and Bertelsmeier, C. (2021) Insect and plant invasions follow two waves of globalisation. *Ecology letters*, **24**, 2418–2426.
- Borgan, O., Goldstein, L. and Langholz, B. (1995) Methods for the analysis of sampled cohort data in the cox proportional hazards model. *The Annals of Statistics*, 1749–1778.
- Borgan, Ø. and Langholz, B. (1997) Risk set sampling designs for proportional hazard models. *Preprint series. Statistical Research Report* <http://urn.nb.no/URN:NBN:no-23420>.
- Borgan, Ø. and Zhang, Y. (2015) Using cumulative sums of martingale residuals for model checking in nested case-control studies. *Biometrics*, **71**, 696–703.
- Boschi, M., Wit, E.-J. C. and Montanari, A. (2022) Relational event models with time varying effects and random effects: an application to the alien species invasions.

- Brandenberger, L. (2019) Predicting network events to assess goodness of fit of relational event models. **27**, 556–571. URL: [https://www.cambridge.org/core/product/identifier/S104719871900010X/type/journal\\_article](https://www.cambridge.org/core/product/identifier/S104719871900010X/type/journal_article).
- Butts, C. T. (2008) 4. a relational event framework for social action. **38**, 155–200. URL: <http://journals.sagepub.com/doi/10.1111/j.1467-9531.2008.00203.x>.
- Calatayud, P., Tertuliano, M. and Le Rü, B. (1994) Seasonal changes in secondary compounds in the phloem sap of cassava in relation to plant genotype and infestation by phenacoccus manihoti (homoptera: Pseudococcidae). *Bulletin of Entomological Research*, **84**, 453–459.
- Cox, D. R. (1975) Partial likelihood. **62**, 269–276. URL: <https://doi.org/10.1093/biomet/62.2.269>. eprint: <https://academic.oup.com/biomet/article-pdf/62/2/269/964098/62-2-269.pdf>.
- Dyer, E. E., Cassey, P., Redding, D. W., Collen, B., Franks, V., Gaston, K. J., Jones, K. E., Kark, S., Orme, C. D. L. and Blackburn, T. M. (2017) The global distribution and drivers of alien bird species richness. *PLoS biology*, **15**, e2000942.
- Hejda, M., Chytrý, M., Pergl, J. and Pyšek, P. (2015) Native-range habitats of invasive plants: are they similar to invaded-range habitats and do they differ according to the geographical direction of invasion? *Diversity and Distributions*, **21**, 312–321.
- Hijmans, R. J., Karney, C., Williams, E. and C., V. (2017) *Package geosphere: Spherical Trigonometry*, 1(7). URL: <https://cran.r-project.org/web/packages/geosphere/index.html>. R package version 1.5-7.
- Hulme, P. E. (2021) Unwelcome exchange: International trade as a direct and indirect driver of biological invasions worldwide. *One Earth*, **4**, 666–679.
- Hurtt, G., Chini, L., Frohking, S., Betts, R., Feddema, J., Fischer, G., Fisk, J., Hibbard, K., Houghton, R., Janetos, A., Jones, C., Kindermann, G., Kinoshita, T., Goldewijk, K. K., Riahi, K. and E (2011) Harmonization of land-use scenarios for the period 1500–2100: 600 years of global gridded annual land-use transitions, wood harvest, and resulting secondary lands. *Climatic Change*, **109**, 117–161. URL: <https://ideas.repec.org/a/spr/climat/v109y2011i1p117-161.html>.
- Juozaitienė, R., Seebens, H., Latombe, G., Essl, F. and Wit, E. C. (2023) Analysing ecological dynamics with relational event models: the case of biological invasions.
- Kirk, W. D. J. and Terry, L. I. (2003) The spread of the western flower thrips *frankliniella occidentalis* (pergande). *Agricultural and Forest Entomology*, **5**, 301–310. URL: <https://resjournals.onlinelibrary.wiley.com/doi/abs/10.1046/j.1461-9563.2003.00192.x>.
- van Kleunen, M., Pyšek, P., Dawson, W., Kreft, H., Pergl, J., Weigelt, P., Stein, A., Dullinger, S., König, C., Lenzner, B. et al. (2019) The global naturalized alien flora (glonaf) database. *Ecology*. 2019; 100: 1.

- Kumar, P. L., Rao, R., Reddy, A., Madhavi, K. J., Anitha, K. and Waliyar, F. (2008) Emergence and spread of tobacco streak virus menace in india and control strategies. *Indian Journal of Plant Protection*, **36**, 1–8.
- Lenzner, B., Latombe, G., Schertler, A., Seebens, H., Yang, Q., Winter, M., Weigelt, P., van Kleunen, M., Pyšek, P., Pergl, J. et al. (2022) Naturalized alien floras still carry the legacy of european colonialism. *Nature Ecology & Evolution*, **6**, 1723–1732.
- Lerner, J. and Lomi, A. (2020) Reliability of relational event model estimates under sampling: How to fit a relational event model to 360 million dyadic events. **8**, 97–135. URL: [https://www.cambridge.org/core/product/identifier/S2050124219000572/type/journal\\_article](https://www.cambridge.org/core/product/identifier/S2050124219000572/type/journal_article).
- Lin, D. Y., Wei, L.-J. and Ying, Z. (1993) Checking the cox model with cumulative sums of martingale-based residuals. *Biometrika*, **80**, 557–572.
- Macharia, I., Backhouse, D., Wu, S.-B. and Ateka, E. M. (2016) Weed species in tomato production and their role as alternate hosts of tomato spotted wilt virus and its vector frankliniella occidentalis. *Annals of Applied Biology*, **169**, 224–235.
- Marzec, L. and Marzec, P. (1997) On fitting cox’s regression model with time-dependent coefficients. *Biometrika*, **84**, 901–908.
- (1998) Testing based on sampled data for proportional hazards model. *Statistics & probability letters*, **37**, 303–313.
- McNeely, J. A. (2001) *Global strategy on invasive alien species*. IUCN.
- Pedersen, E. J., Miller, D. L., Simpson, G. L. and Ross, N. (2019) Hierarchical generalized additive models in ecology: an introduction with mgcv. *PeerJ*, **7**, e6876.
- Perry, P. O. and Wolfe, P. J. (2013) Point process modelling for directed interaction networks. **75**, 821–849. URL: <https://onlinelibrary.wiley.com/doi/10.1111/rssb.12013>.
- Prior, K. M., Robinson, J. M., Meadley Dunphy, S. A. and Frederickson, M. E. (2015) Mutualism between co-introduced species facilitates invasion and alters plant community structure. *Proceedings of the Royal Society B: Biological Sciences*, **282**, 20142846.
- Pyšek, P., Bacher, S., Chytrý, M., Jarošík, V., Wild, J., Celesti-Grappo, L., Gassó, N., Kenis, M., Lambdon, P. W., Nentwig, W. et al. (2010) Contrasting patterns in the invasions of european terrestrial and freshwater habitats by alien plants, insects and vertebrates. *Global ecology and biogeography*, **19**, 317–331.
- Pyšek, P., Hulme, P. E., Simberloff, D., Bacher, S., Blackburn, T. M., Carlton, J. T., Dawson, W., Essl, F., Foxcroft, L. C., Genovesi, P. et al. (2020) Scientists’ warning on invasive alien species. *Biological Reviews*, **95**, 1511–1534.
- Pyšek, P. and Richardson, D. M. (2010) Invasive species, environmental change and management, and health. *Annual Review of Environment and Resources*, **35**, 25–55. URL: <https://doi.org/10.1146/annurev-environ-033009-095548>.

- Richardson, D. M., Allsopp, N., D'ANTONIO, C. M., Milton, S. J. and Rejmánek, M. (2000) Plant invasions—the role of mutualisms. *Biological Reviews*, **75**, 65–93.
- Seebens, H., Blackburn, T. M., Dyer, E. E., Genovesi, P., Hulme, P. E., Jeschke, J. M., Pagad, S., Pyšek, P., van Kleunen, M., Winter, M. et al. (2018) Global rise in emerging alien species results from increased accessibility of new source pools. *Proceedings of the National Academy of Sciences*, **115**, E2264–E2273.
- Seebens, H., Blackburn, T. M., Dyer, E. E., Genovesi, P., Hulme, P. E., Jeschke, J. M., Pagad, S., Pyšek, P., Winter, M., Arianoutsou, M. et al. (2017) No saturation in the accumulation of alien species worldwide. *Nature communications*, **8**, 1–9.
- Seebens, H., Blackburn, T. M., Hulme, P. E., van Kleunen, M., Liebhold, A. M., Orlova-Bienkowskaja, M., Pyšek, P., Schindler, S. and Essl, F. (2021) Around the world in 500 years: Inter-regional spread of alien species over recent centuries. *Global Ecology and Biogeography*, **30**, 1621–1632.
- Simberloff, D. and Von Holle, B. (1999) Positive interactions of nonindigenous species: invasional meltdown? *Biological invasions*, **1**, 21–32.
- Vu, D., Lomi, A., Mascia, D. and Pallotti, F. (2017) Relational event models for longitudinal network data with an application to interhospital patient transfers. **36**, 2265–2287. URL: <https://onlinelibrary.wiley.com/doi/10.1002/sim.7247>.
- Walliser, J. (2013) *Attracting Beneficial Bugs to Your Garden: A Natural Approach to Pest Control*. Timber Press.
- Watanabe, S., Hajima, T., Sudo, K., Nagashima, T., Takemura, T., Okajima, H., Nozawa, T., Kawase, H., Abe, M., Yokohata, T. et al. (2011) Miroc-esm 2010: Model description and basic results of cmip5-20c3m experiments. *Geoscientific Model Development*, **4**, 845–872.
- Wood, S. N. (2003) Thin-plate regression splines. *Journal of the Royal Statistical Society (B)*, **65**, 95–114.
- (2017) Generalized additive models: An introduction with r. 397.
- Wood, S. N., Pya, N. and Säfken, B. (2016) Smoothing parameter and model selection for general smooth models. *Journal of the American Statistical Association*, **111**, 1548–1563. URL: <https://doi.org/10.1080/01621459.2016.1180986>.

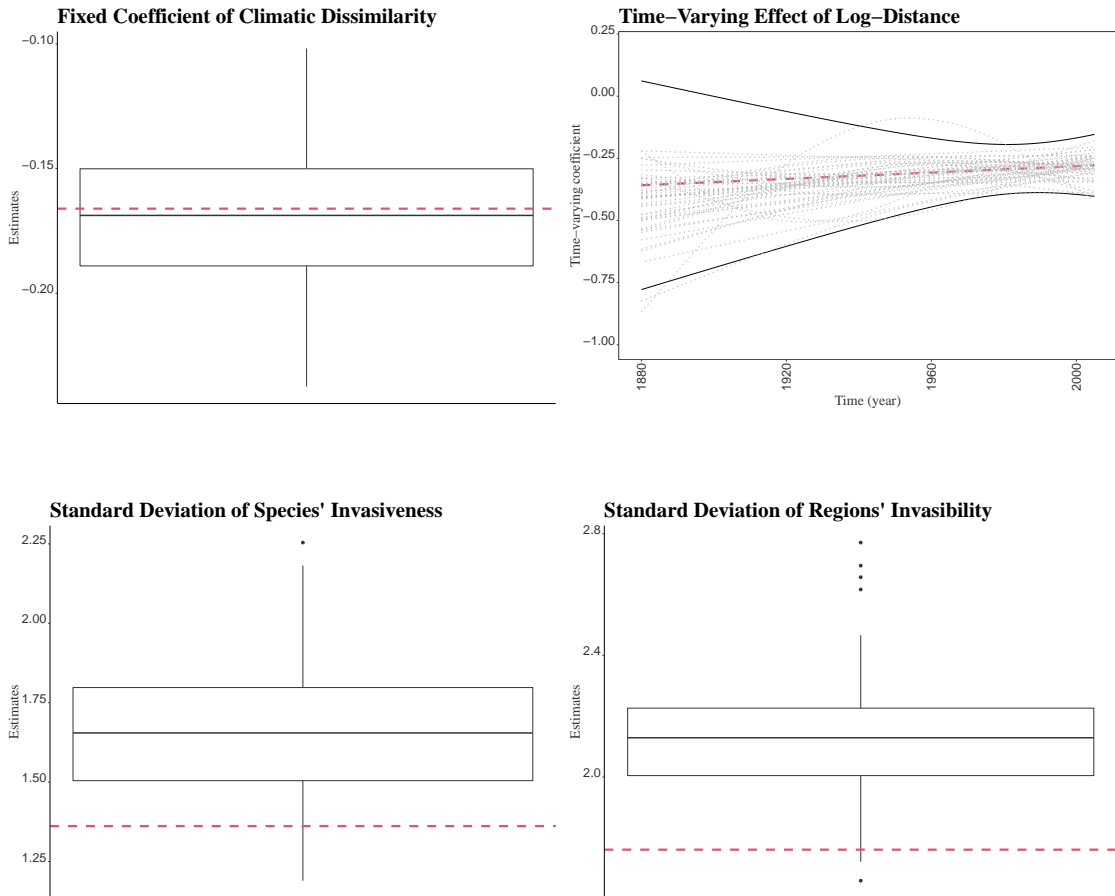


**Figure 1.** Comparison between the true value leading the underlying intensity (red dashed lines) and the estimates deriving from the fitting to the simulated data. Particularly: *Up-right* Estimates for the fixed effect of *Climatic Dissimilarity* are reported in the boxplot; *Up-left* Estimates for the time-varying effect of *Distance* are reported in the dotted gray lines; *Bottom* Estimates for the standard deviation of the random effects are reported in the boxplots.

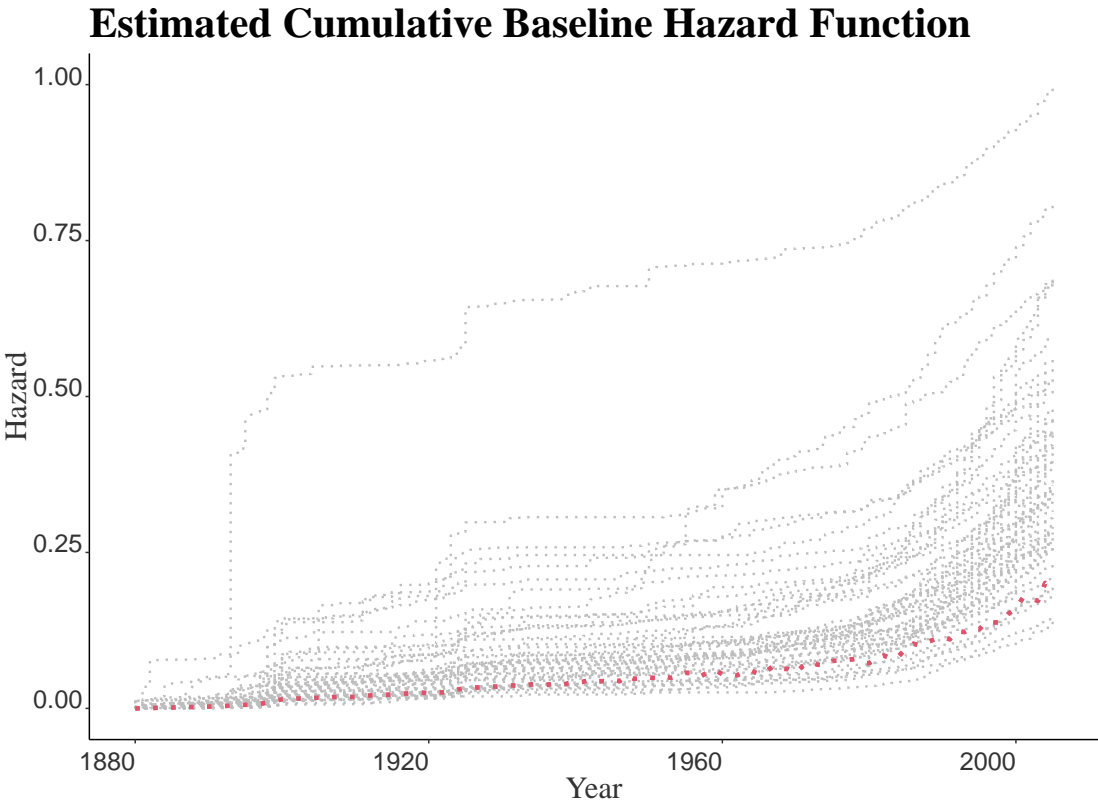


**Figure 2.** Comparison between the true (red dashed line) and the non-parametric estimates (gray dotted lines) of the cumulative baseline hazard.

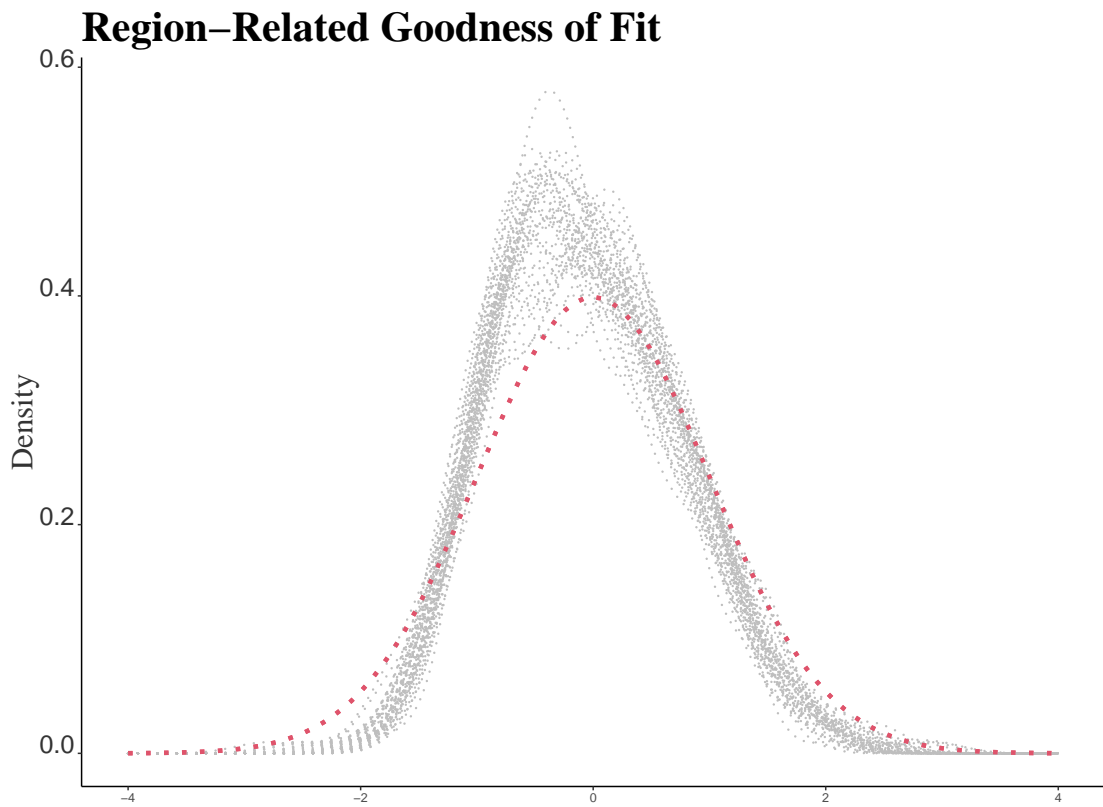


**Figure 3.** Evaluation of the Goodness of Fit of the Smooth REM on Simulated Data. Densities of the computed test statistic on the involved regions (gray dotted lines) are compared to the Gaussian density (red dashed line).



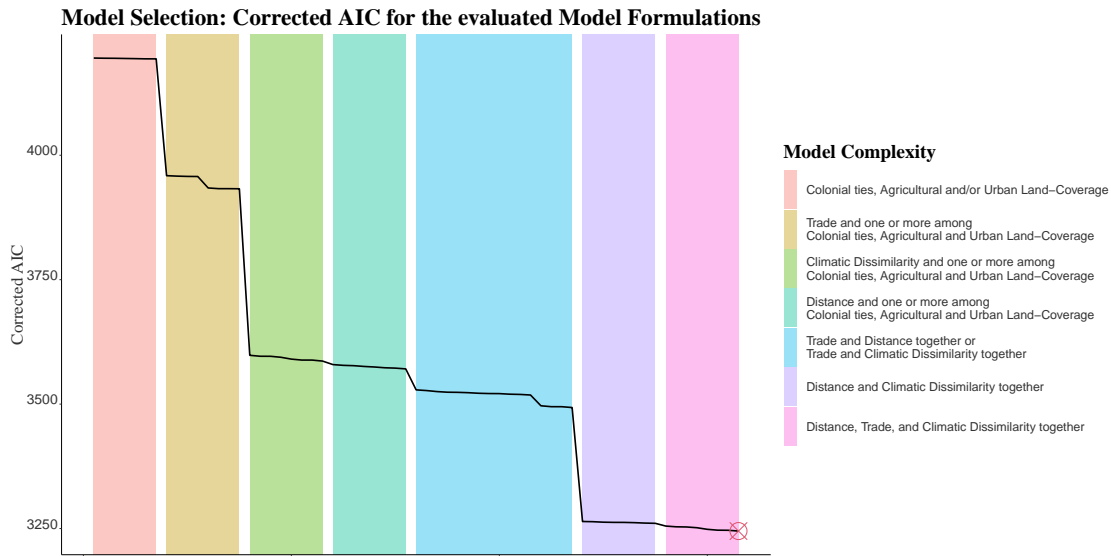


**Figure 4.** Corrected Values of AIC for the examined model formulations. We outline that, whenever included, *Distance*, *Trade*, and *Agricultural Land-Coverage* are supposed to have a time-varying impact while *Climatic Dissimilarity*, *Urban Land-Coverage*, and *Colonial Ties* a fixed effect. This choice come from the previous studies on the topic (Juozaitienė et al., 2023). On the other side, all the considered models include random effects for species invasiveness, region invasibility and species co-invasion. The best model in terms of corrected AIC (Wood et al., 2016) includes *Distance*, *Trade*, *Colonial Ties* and *Climatic Dissimilarity* and is outlined in the plot with a red crossed symbol. According to the covariates included in the compared models, we can distinguish seven groups of model formulations.

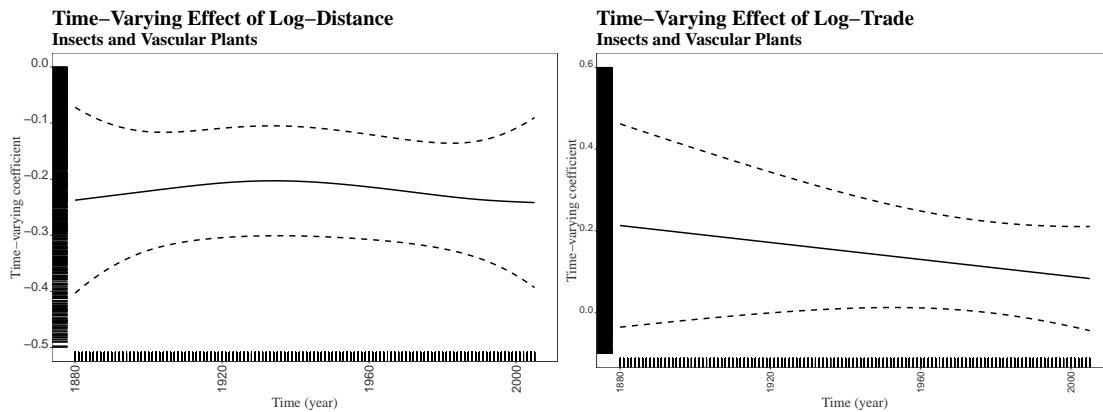


**Figure 5.** Time-Varying Coefficients for *Distance* and *Trade* (continuous lines) with the related posterior confidence intervals (dotted lines).

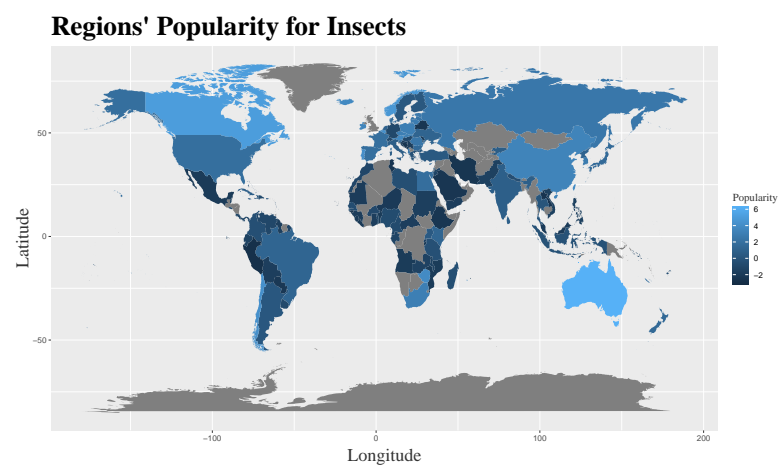


**Figure 6.** Regions' invasibility in terms of estimated random effects. Lightest-blue areas are those that the model identifies as most popular, such as Australia and Canada. On the other hand, darker locations are those that lead to a decrease in the rate of occurrence of alien species invasions (Peru and Saudi Arabia are some instances).

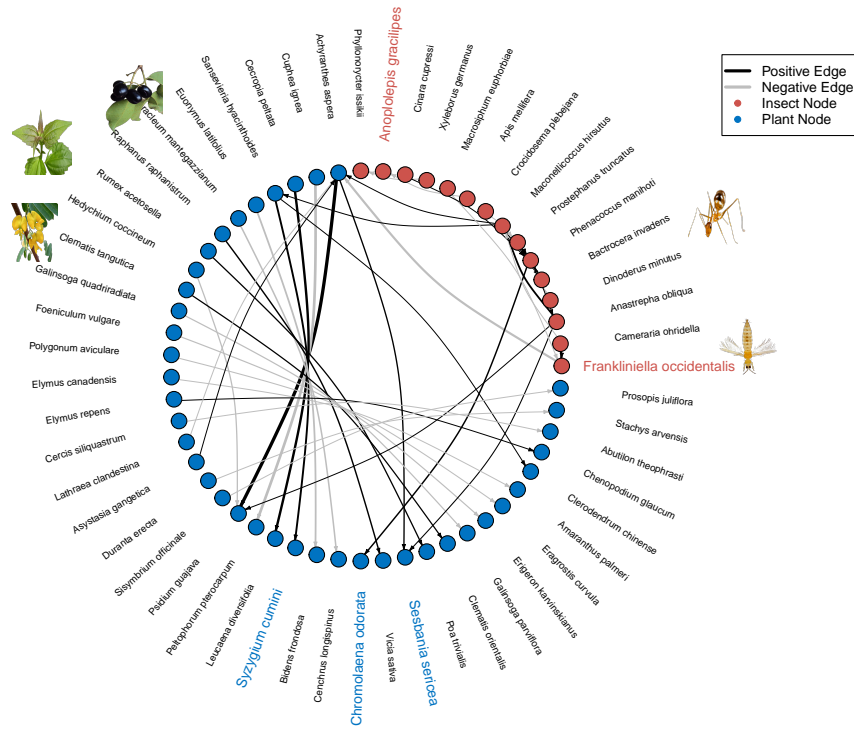


**Figure 7.** Strongest associations between species in terms of co-invasion. We report here the values that are larger or equal, in absolute value, than the logarithm of 1.5. Taking into account all the other features, the presence of the linked species-last species coinvasion lead to increasing or decreasing the risk of invasion at least of 50%. The taxonomy determines the colour of the nodes (blue for plants and red for insects). When the estimated random coefficient is positive, the link is shown in black; a positive link indicates a higher probability of the sender node following the receiver node, meaning the risk for the sender species of entering a nation that has just been invaded by the recipient species in the plot is increased. The thicker the edge, the larger (in absolute value) the estimate for the corresponding random effect. The figures represent the nodes with the largest values in terms of species invasiveness.

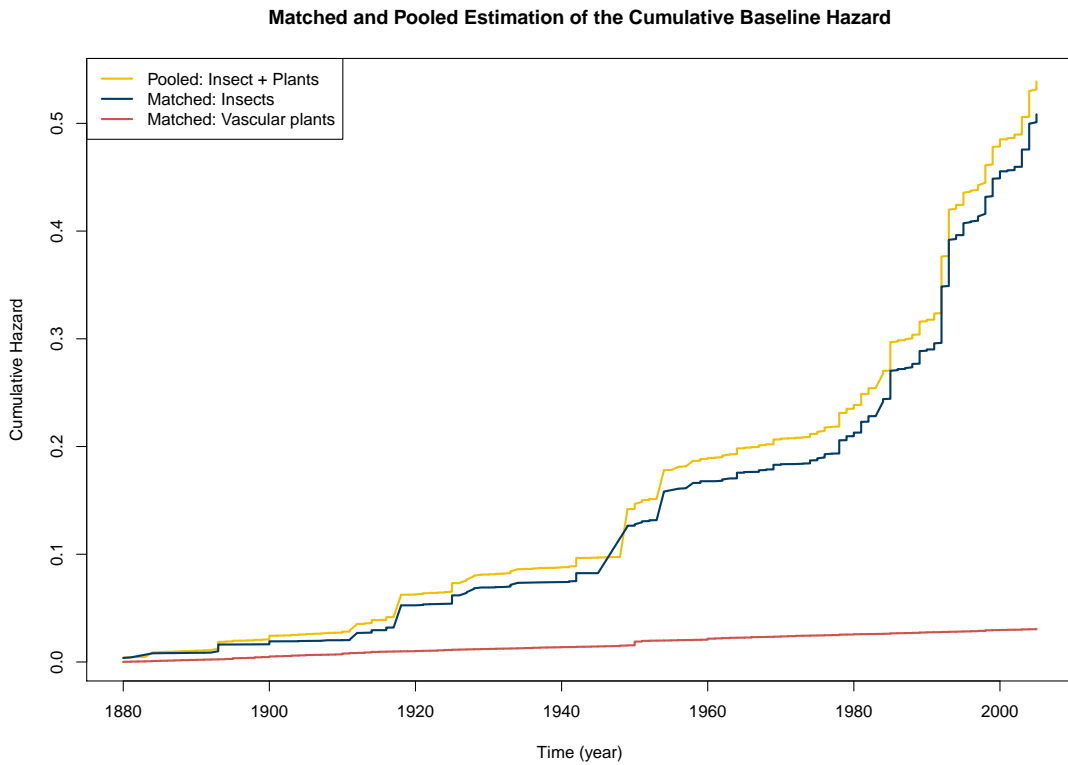


**Figure 8.** Matched and Pooled Estimates of the Cumulative Baseline Hazard. Following Borgan and Langholz (1997), we may provide a taxa-specific estimate of the baseline (blue for insects, red for plants); as an alternative, we may rely on a pooled estimate (yellow line) that takes into account the fact that the sampled control belongs to the same group as the observed case.